hexagon:2611.00647v1

Fourier Epicycles and Antisymmetric Signed-Area Conservation in Normalized Riemann Zeta Terms

Ryan Hackbarth
hackbarthr16@hanover.edu

November 19, 2026

Abstract

In companion studies of Euler's alternating series $\eta(s) = (1-2^{1-s})\zeta(s)$ and its prime-base normalizations $\eta_p(s) = (1-p^{1-s})\zeta(s)$, distributing the prefactor $(1-p^{1-s})^{-1}$ across individual summands $t_{p,n}(s) = c_p(n)(1-p^{1-s})^{-1}n^{-s}$ exposed an infinite hierarchy of closed, irreducible degree-$2k$ plane algebraic curves $t_{p,p^k}(\frac{1}{2}+ib)$ over $\mathbb{Z}[x,y]$ on the critical line $\mathrm{Re}(s) = \frac{1}{2}$, whose enclosed signed areas satisfy $\mathcal{A}_{\text{signed}}(t_4) = 0$ at the base-2 Bernoulli lemniscate and $\sum_{k=1}^{\infty}\mathcal{A}_{\text{signed}}(t_{p,p^k}) = 0$ across every prime tower. Rather than keeping $(1-p^{1-s})^{-1}$ unexpanded to preserve Cartesian curve equations, this paper expands $(1-p^{1-s})^{-1} = -\sum_{m=1}^{\infty}p^{m(s-1)}$ across the critical strip $0 < \mathrm{Re}(s) < 1$ and distributes it termwise as a Fourier epicycle series. For every pure power $n = p^k$ $(k \geq 1)$ along $s = a+ib$, the distributed expansion separates into $k-1$ clockwise circles $(1 \leq m \leq k-1)$, a motionless center-of-mass anchor $+(p-1)p^{-k}$ $(m = k)$ independent of s, and an infinite counterclockwise tail $(m \geq k+1)$, revealing index-by-index how counter-rotating harmonics fold and area-balance the Lemniscate of Bernoulli $t_4(\frac{1}{2}+ib)$. Evaluating Green's theorem via Parseval's identity yields an exact closed-form signed-area formula for $t_{p,p^k}(a+ib)$ across $0 < a < 1$, proving that $t_4(a+ib)$ encloses zero net signed area if and only if $a = \frac{1}{2}$—tipping toward its clockwise left lobe for $0 < a < \frac{1}{2}$ and its counterclockwise right lobe for $\frac{1}{2} < a < 1$. Summing over $k \geq 1$ further proves that the total pure-power signed area $\mathcal{S}_p(a)$ is strictly antisymmetric across the critical line $(\mathcal{S}_p(1-a) = -\mathcal{S}_p(a))$, negative on $0 < a < \frac{1}{2}$, positive on $\frac{1}{2} < a < 1$, and zero if and only if $\mathrm{Re}(s) = \frac{1}{2}$.

1 Introduction and Critical-Line Launch Point

The Dirichlet eta function $\eta(s) = (1-2^{1-s})\zeta(s)$ provides the classical analytic continuation of the Riemann zeta function $\zeta(s)$ across the critical strip $0 < \mathrm{Re}(s) < 1$, and extends naturally to any prime base p through the balanced Dirichlet series [1, 2, 3, 7, 12]:

$$\zeta(s) = \frac{\eta_p(s)}{1-p^{1-s}}, \qquad \eta_p(s) = \sum_{n=1}^{\infty}\frac{c_p(n)}{n^s}, \qquad c_p(n) = \begin{cases} 1, & p \nmid n, \\ -(p-1), & p \mid n. \end{cases} \tag{1}$$

In two companion studies [6, 7], distributing the normalizing prefactor $(1-p^{1-s})^{-1}$ directly into each summand defined the normalized term sequence (with $t_n(s) := t_{2,n}(s)$ in base 2):

$$t_{p,n}(s) = \frac{c_p(n)}{(1-p^{1-s})n^s}, \qquad s = a+ib \quad (a \in (0,1)). \tag{2}$$

Keeping the denominator $(1-p^{1-s})$ intact inside Equation (2) exposed a sharp geometric division on the critical line $\mathrm{Re}(s) = \frac{1}{2}$. Weighting non-power indices $(n \neq p^k)$ by $(1-p^{-s})$ collapses precessing trajectories into concentric origin-centered circles of constant radius $|c_p(n)|/\sqrt{pn}$ uniquely at $a = \frac{1}{2}$ [4, 6, 7, 11]. Meanwhile, the pure-power terms $t_{p,p^k}(\frac{1}{2}+ib)$ $(k \geq 1)$ trace closed, irreducible plane algebraic curves of degree $2k$ over $\mathbb{Z}[x,y]$ whose rational Cartesian equations single

out $a = \frac{1}{2}$ among rational abscissas $a \in (0,1) \cap \mathbb{Q}$, anchored in base 2 at $k = 2$ by the Lemniscate of Bernoulli $t_4(\frac{1}{2} + ib)$ [6, 7, 8, 10].

At the close of those critical-line analyses, the pure-power hierarchy exhibited an exact oriented-area conservation law [6, 7]: parameterized by $\theta = b \ln p \in [0, 2\pi]$, each curve $t_{p,p^k}(\frac{1}{2} + ib)$ $(k \geq 1)$ encloses the signed area

$$\mathcal{A}_{\text{signed}}\left(t_{p,p^k}\left(\frac{1}{2} + ib\right)\right) = \frac{p - k(p-1)}{p^k}\,\pi, \qquad \sum_{k=1}^{\infty} \mathcal{A}_{\text{signed}}\left(t_{p,p^k}\left(\frac{1}{2} + ib\right)\right) = 0. \tag{3}$$

On $\mathrm{Re}(s) = \frac{1}{2}$, Equation (3) vanishes individually among all primes and powers solely at $p = 2, k = 2$ $(\mathcal{A}_{\text{signed}}(t_4) = 0)$, while across every prime tower $p \geq 2$ the positive area of the base circle $t_{p,p}$ $(k = 1)$ balances the negative areas of all higher inner-looped curves $(k \geq 2)$.

Equation (3) serves as our launch point here. Because those earlier derivations worked primarily on $\mathrm{Re}(s) = \frac{1}{2}$ while keeping $(1 - p^{1-s})^{-1}$ unexpanded to preserve algebraic curve equations, they left open how the enclosed signed areas behave on off-critical vertical lines $a \neq \frac{1}{2}$. In Section 2, we expand $(1 - p^{1-s})^{-1}$ as a convergent exterior power series across $0 < \mathrm{Re}(s) < 1$ and distribute it across the summands of $\eta_p(s)$. Although termwise expansion dissolves individual closed algebraic curves into uniform-speed circles, viewing the distributed sum as a Fourier epicycle decomposition separates every pure-power curve $t_{p,p^k}(a + ib)$ into finite clockwise rotors, a motionless real-axis anchor, and an infinite counterclockwise tail, illuminating index-by-index how the Bernoulli lemniscate $t_4(\frac{1}{2} + ib)$ is assembled. In Section 3, we apply Parseval's area identity to derive closed-form strip-wide formulas for $\mathcal{A}_{\text{signed}}(t_{p,p^k}(a + ib))$ and its tower sum $\mathcal{S}_p(a)$, proving that both the lobe balance of $t_4(a + ib)$ and prime-tower signed-area conservation hold if and only if $\mathrm{Re}(s) = \frac{1}{2}$, with strict antisymmetry under $a \leftrightarrow 1 - a$.

2 Exterior Power-Series Distribution and Fourier Epicycle Decomposition

2.1 Convergent Strip Expansion and Termwise Epicycle Splitting

To represent the normalizing prefactor $(1 - p^{1-s})^{-1}$ as a convergent power series on vertical lines $s = a + ib$ inside the critical strip $0 < a < 1$, observe that the naive geometric variable $u = p^{1-s}$ has modulus $|u| = p^{1-a} > 1$ throughout $0 < a < 1$ and therefore lies strictly outside the unit Maclaurin disk $|u| < 1$. Likewise, rational substitutions around a fixed center—such as writing $\eta(s) = \frac{x}{1-x}\zeta(s)$ with $x(s) = \frac{1-2^{1-s}}{2-2^{1-s}}$ and expanding $\frac{1-x}{x} = \sum_{m=1}^{\infty}(1-x)^m$—cannot converge uniformly along $a = \frac{1}{2}$: on the critical line, $x(\frac{1}{2} + ib)$ traces the origin-centered circle $|x| = \frac{1}{\sqrt{2}}$ enclosing the pole $x = 0$ of $\frac{1-x}{x}$, forcing $|1 - x(\frac{1}{2} + ib)| = (6 - 4\sqrt{2}\cos(b \ln 2))^{-1/2}$ to exceed 1 whenever $\cos(b \ln 2) \geq \frac{5\sqrt{2}}{8}$.

Inverting $u = p^{1-s}$ into the exterior Laurent variable $y := u^{-1} = p^{s-1}$ moves the pole $y = 1$ outside the trajectory across the entire strip $0 < a < 1$, since $|y| = p^{a-1} < 1$ is independent of the ordinate b (with constant modulus $p^{-1/2} < 1$ everywhere on $a = \frac{1}{2}$). Factoring $-p^{1-s}$ from the denominator yields the uniformly convergent strip power series

$$\frac{1}{1 - p^{1-s}} = -\frac{p^{s-1}}{1 - p^{s-1}} = -\sum_{m=1}^{\infty} p^{m(s-1)} \qquad (0 < \mathrm{Re}(s) < 1), \tag{4}$$

expressing $\zeta(s)$ across $0 < \mathrm{Re}(s) < 1$ as the convergent product

$$\zeta(s) = -\left(\sum_{m=1}^{\infty} p^{m(s-1)}\right)\left(\sum_{n=1}^{\infty} \frac{c_p(n)}{n^s}\right). \tag{5}$$

Because $\eta_p(s)$ converges only conditionally on $0 < \mathrm{Re}(s) < 1$, the outer and inner summations in Equation (5) cannot be interchanged globally across all $n \in \mathbb{N}$ at once. Distributing the m-series into each individual summand $c_p(n)n^{-s}$, however, converges absolutely and uniformly in $b \in \mathbb{R}$ for every fixed $n \geq 1$ and $a \in (0,1)$:

$$t_{p,n}(a+ib) = \sum_{m=1}^{\infty} u_{p;n,m}(a+ib), \qquad u_{p;n,m}(a+ib) := -c_p(n)\, p^{-m(1-a)} n^{-a} e^{ib(m\ln p - \ln n)}. \tag{6}$$

Viewed geometrically as b varies, Equation (6) trades single algebraic equations for a superposition of uniform-speed circular rotors:

- **Non-Power Indices ($n \neq p^k$):** Since $p^m \neq n$ for every $m \geq 1$, the angular velocity $m\ln p - \ln n$ never vanishes. Every sub-term $u_{p;n,m}(a+ib)$ traces an origin-centered circle of radius $|c_p(n)|p^{-m(1-a)}n^{-a}$, and the curve's time-averaged center of mass $\lim_{T\to\infty} \frac{1}{2T}\int_{-T}^{T} t_{p,n}(a+ib)\, db$ equals 0 across all $a \in (0,1)$.
- **Pure-Power Indices ($n = p^k$, $k \geq 1$):** Here $-c_p(p^k) = p-1$ and $m\ln p - \ln(p^k) = (m-k)\ln p$. Setting $\theta = b\ln p \in [0, 2\pi]$ locks all harmonics to integer multiples of a single fundamental frequency, partitioning $t_{p,p^k}(a+ib)$ into three distinct kinematic components:

$$\begin{aligned} t_{p,p^k}(a+ib) = {} & \underbrace{(p-1)\sum_{m=1}^{k-1} p^{-m(1-a)-ka} e^{-i(k-m)\theta}}_{k-1 \text{ clockwise circles } (m<k)} + \underbrace{\frac{p-1}{p^k}}_{\substack{\text{static anchor} \\ (m=k)}} \\ & + \underbrace{(p-1)\sum_{m=k+1}^{\infty} p^{-m(1-a)-ka} e^{+i(m-k)\theta}}_{\text{infinite counterclockwise tail } (m>k)}. \end{aligned} \tag{7}$$

Remarkably, at the resonant diagonal index $m = k$ ($p^m = p^k$), both the ordinate phase $(m-k)b\ln p$ and the abscissa a cancel out of $-c_p(p^k)p^{-k(1-a)-ka} = (p-1)p^{-k}$. Every pure-power curve $t_{p,p^k}(a+ib)$ therefore possesses an s-invariant time-averaged center of mass at $\left(+\frac{p-1}{p^k}, 0\right)$ across the entire strip $0 < a < 1$ (summing over $k \geq 1$ to $+1$). In base 2, this places the mean position of $t_2(\frac{1}{2}+ib)$ at $(+\frac{1}{2}, 0)$ and of $t_4(\frac{1}{2}+ib)$ at $(+\frac{1}{4}, 0)$, shifted left of their geometric centers $(+1, 0)$ and $(+\frac{1}{2}, 0)$ because non-uniform Blaschke speed lingers near periapsis ($\theta = \pi$) and whips rapidly past apoapsis ($\theta = 0$) [6].

2.2 Index-by-Index Construction of the Bernoulli Lemniscate $t_4(\frac{1}{2}+ib)$

Evaluating Equation (7) at $p = 2$, $k = 2$, and $a = \frac{1}{2}$ ($\theta = b\ln 2$) exposes the internal Fourier epicycle structure of the Lemniscate of Bernoulli $t_4(\frac{1}{2}+ib)$:

$$t_4\left(\frac{1}{2}+ib\right) = \underbrace{\frac{1}{2\sqrt{2}}e^{-i\theta}}_{\text{CW } (m=1)} + \underbrace{\frac{1}{4}}_{\substack{\text{anchor} \\ (m=2)}} + \underbrace{\frac{1}{4\sqrt{2}}e^{+i\theta} + \frac{1}{8}e^{+2i\theta} + \frac{1}{8\sqrt{2}}e^{+3i\theta} + \cdots}_{\text{CCW tail } (m\geq 3)}. \tag{8}$$

Adding the harmonics of Equation (8) sequentially by index m reveals how uniform-speed circles fold into a zero-area figure-eight:

1. **Anchor and Clockwise Rotor ($m = 1, 2$):** Starting from the motionless $m = 2$ anchor at $(+\frac{1}{4}, 0)$, the $m = 1$ harmonic attaches a single clockwise circle ($\omega = -1$) of radius $\frac{1}{2\sqrt{2}} \approx 0.3536$, enclosing negative signed area $-\pi\left(\frac{1}{2\sqrt{2}}\right)^2 = -\frac{\pi}{8}$.

2. **First Counterclockwise Rotor ($+m = 3$):** Adding $\frac{1}{4\sqrt{2}}e^{+i\theta}$ ($\omega = +1$) couples two opposite-spinning circles of equal speed around $(+\frac{1}{4}, 0)$. Their horizontal components reinforce to semi-axis $\frac{3}{4\sqrt{2}} \approx 0.5303$ while their vertical components partially cancel to semi-axis $\frac{1}{4\sqrt{2}} \approx 0.1768$, flattening the circle into a clockwise ellipse of net signed area $-\frac{\pi}{8} + \frac{\pi}{32} = -\frac{3\pi}{32}$.

3. **Second Counterclockwise Rotor ($+m = 4$):** Attaching the double-speed rotor $\frac{1}{8}e^{+2i\theta}$ ($\omega = +2$) pulls the right arc outward at $\theta = 0, \pi$ while pinching the vertical waist across the real axis near $\theta = \pm\frac{\pi}{4}$, producing the first self-crossing figure-eight of net signed area $-\frac{3\pi}{32} + 2 \cdot \frac{\pi}{64} = -\frac{\pi}{16}$.

4. **Full Counterclockwise Tail ($m \geq 3$):** Each harmonic $m = 2 + j$ ($j \geq 1$) has radius $2^{-(j+4)/2}$ and winding $+j$, contributing positive signed area $+j\pi\, 2^{-(j+4)} = \frac{\pi}{32}\, j\, 2^{-(j-1)}$. Although every individual counterclockwise circle is smaller than the $m = 1$ clockwise circle, their faster winding numbers amplify their area contributions so that

$$\mathcal{A}_{\mathrm{CCW}} = \frac{\pi}{32} \sum_{j=1}^{\infty} j\, 2^{-(j-1)} = \frac{\pi}{32} \cdot \frac{1}{(1-\frac{1}{2})^2} = +\frac{\pi}{8}, \tag{9}$$

canceling $\mathcal{A}_{\mathrm{CW}} = -\frac{\pi}{8}$ identically to close the curve into the symmetric Bernoulli lemniscate spanning $\big[-\frac{\sqrt{2}-1}{2}, \frac{\sqrt{2}+1}{2}\big]$ on the real axis with self-intersection node at $(+\frac{1}{2}, 0)$ [6, 10].

3 Strip-Wide Signed-Area Law and Critical-Line Antisymmetry

3.1 Closed-Form Signed Area of $t_{p,p^k}(a+ib)$ and Lobe Tipping of $t_4(a+ib)$

Moving off the critical line ($a \neq \frac{1}{2}$) rescales the clockwise and counterclockwise radii in Equation (7) asymmetrically through $p^{-m(1-a)-ka}$, tipping the area balance between opposite-spinning rotors. Applying Hurwitz's and Gronwall's classical Fourier–Green area formula [5, 9] across $0 < a < 1$ yields an exact closed form for every pure-power curve.

Theorem 3.1 (Strip-Wide Signed-Area Formula and Uniqueness of t_4)**.** *For every integer base $p \geq 2$, exponent $k \geq 1$, and abscissa $a \in (0,1)$, the closed curve $\theta \mapsto t_{p,p^k}(a+ib)$ ($\theta = b \ln p \in [0, 2\pi]$) encloses the oriented signed area*

$$\mathcal{A}_{\mathrm{signed}}\big(t_{p,p^k}(a+ib)\big) = \frac{\pi(p-1)^2\, p^{-2ka}\, p^{2a-2}}{\big(1-p^{2a-2}\big)^2}\Big(1 - k\big(1-p^{2a-2}\big)\Big). \tag{10}$$

In particular, for $p = 2$ and $k = 2$, the figure-eight curve $t_4(a+ib)$ crosses itself on the real axis at $x_{\mathrm{node}}(a) = 4^{-a}$ ($\cos\theta = 2^{-a}$) for every $a \in (0,1)$, and its enclosed signed area

$$\mathcal{A}_{\mathrm{signed}}\big(t_4(a+ib)\big) = \frac{\pi\, 4^{-a-1}\big(2 \cdot 4^{a-1} - 1\big)}{\big(1-4^{a-1}\big)^2} \tag{11}$$

is strictly negative for $0 < a < \frac{1}{2}$, strictly positive for $\frac{1}{2} < a < 1$, and vanishes if and only if $a = \frac{1}{2}$.

Proof. For fixed $a \in (0,1)$, the Fourier series $t_{p,p^k}(a+ib) = \sum_{m=1}^{\infty} c_{k,m}(a) e^{i(m-k)\theta}$ in Equation (7) has coefficients $c_{k,m}(a) = (p-1)p^{-m(1-a)-ka}$, which decay exponentially as $O(p^{-m(1-a)})$ since $1 - a > 0$. Termwise differentiation with respect to θ is therefore uniformly valid, and Green's theorem combined with $L^2([0, 2\pi])$ orthogonality of $\{e^{in\theta}\}_{n\in\mathbb{Z}}$ [5, 9] gives

$$\begin{aligned} \mathcal{A}_{\mathrm{signed}}\big(t_{p,p^k}(a+ib)\big) &= \frac{1}{2}\int_0^{2\pi} \mathrm{Im}\left(\overline{t_{p,p^k}(a+ib)}\, \frac{\partial t_{p,p^k}(a+ib)}{\partial\theta}\right) d\theta \\ &= \pi \sum_{m=1}^{\infty} (m-k)\, \big|c_{k,m}(a)\big|^2 = \pi(p-1)^2 p^{-2ka} \sum_{m=1}^{\infty} (m-k)\, q^m, \end{aligned} \tag{12}$$

where $q := p^{-2(1-a)} = p^{2a-2} \in (p^{-2}, 1)$ for $a \in (0,1)$. Substituting the convergent geometric sums $\sum_{m=1}^{\infty} m\, q^m = \frac{q}{(1-q)^2}$ and $\sum_{m=1}^{\infty} q^m = \frac{q}{1-q}$ into Equation (12) yields

$$\pi(p-1)^2 p^{-2ka}\left(\frac{q}{(1-q)^2} - \frac{k\,q}{1-q}\right) = \frac{\pi(p-1)^2 p^{-2ka}\, q}{(1-q)^2}\big(1-k(1-q)\big),$$

establishing Equation (10) (which reduces at $a = \frac{1}{2}$, $q = p^{-1}$, to $\frac{p-k(p-1)}{p^k}\pi$ in Equation (3)).

Setting $p = 2$, $k = 2$, and $z = e^{-i\theta}$ in $t_4(a+ib) = -4^{-a}z^2(1-2^{1-a}z)^{-1}$, multiplying numerator and denominator by $1 - 2^{1-a}\bar{z}$ gives

$$\operatorname{Im} t_4(a+ib) = \frac{4^{-a}\sin\theta\,\big(2\cos\theta - 2^{1-a}\big)}{1 + 4^{1-a} - 2^{2-a}\cos\theta}.$$

Since $2^{1-a}/2 = 2^{-a} \in (\frac{1}{2}, 1)$ for all $a \in (0,1)$, $\operatorname{Im} t_4(a+ib) = 0$ occurs at the periapsis $\theta = \pi$, the apoapsis $\theta = 0$, and the non-tangential self-intersection pair $\theta = \pm\arccos(2^{-a})$, where

$$t_4\big(a + i\theta/\ln 2\big)\Big|_{\cos\theta = 2^{-a}} = \frac{-4^{-a}\big(\cos 2\theta - 2^{1-a}\cos\theta\big)}{1 + 4^{1-a} - 2^{2-a}(2^{-a})} = \frac{-4^{-a}\big(2\cdot 4^{-a} - 1 - 2\cdot 4^{-a}\big)}{1} = 4^{-a}.$$

Evaluating Equation (10) at $p = 2, k = 2$ ($q = 4^{a-1}$) gives Equation (11), whose sign is governed by $2\cdot 4^{a-1} - 1 = 2^{2a-1} - 1$, which is negative on $(0, \frac{1}{2})$, positive on $(\frac{1}{2}, 1)$, and zero uniquely at $a = \frac{1}{2}$. □

Figure 1 illustrates Theorem 3.1 across $a \in \{0.25, 0.50, 0.75\}$. While the $m = 2$ Fourier anchor stays fixed at $(+\frac{1}{4}, 0)$ across all three panels, increasing a slides the self-intersection node $x_{\text{node}}(a) = 4^{-a}$ leftward from $+0.707$ ($a = 0.25$, clockwise left lobe dominant) through $+0.500$ ($a = \frac{1}{2}$, congruent Bernoulli lemniscate lobes) to $+0.354$ ($a = 0.75$, counterclockwise right lobe dominant).

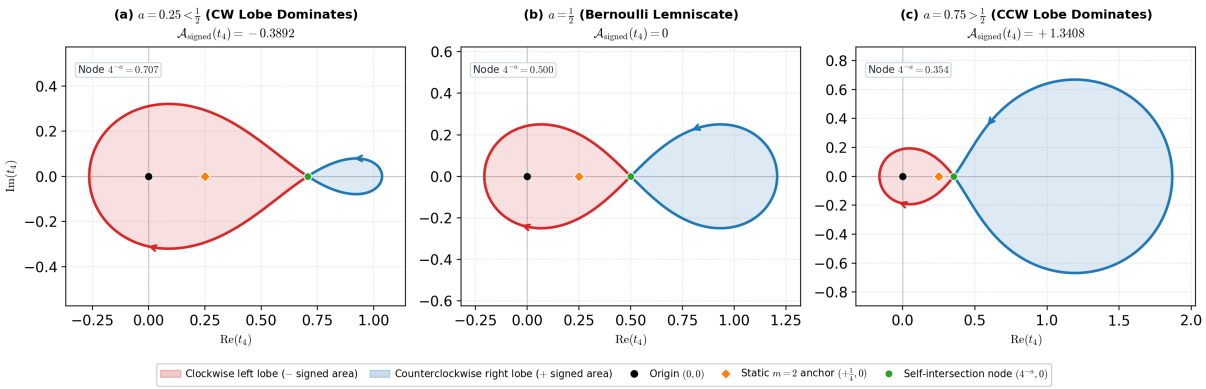


Figure 1: Off-critical lobe tipping and enclosed signed area of $t_4(a+ib)$ across $0 < a < 1$: (a) at $a = 0.25 < \frac{1}{2}$, the self-intersection node sits at $(4^{-0.25}, 0) \approx (+0.707, 0)$ and the clockwise left lobe dominates ($\mathcal{A}_{\text{signed}} \approx -0.3892$); (b) on the critical line $a = \frac{1}{2}$, the node lands at $(+0.500, 0)$, balancing both lobes into a Lemniscate of Bernoulli ($\mathcal{A}_{\text{signed}} = 0$) while the $m = 2$ Fourier anchor remains at $(+\frac{1}{4}, 0)$; and (c) at $a = 0.75 > \frac{1}{2}$, the node retreats to $(4^{-0.75}, 0) \approx (+0.354, 0)$ and the counterclockwise right lobe dominates ($\mathcal{A}_{\text{signed}} \approx +1.3408$).

3.2 Antisymmetric Zero-Crossing Across Prime Towers

For odd primes $p \geq 3$, $1 - k(1-p^{-1}) = 0$ solves to $k = \frac{p}{p-1} \notin \mathbb{Z}$, so no single curve $t_{p,p^k}(\frac{1}{2} + ib)$ encloses zero area on the critical line [7]. Summing Theorem 3.1 across the full pure-power tower $k \geq 1$, however, extends the critical-line conservation law (3) to an antisymmetric characterization of $\operatorname{Re}(s) = \frac{1}{2}$ valid for every base $p \geq 2$ (Figure 2).

Corollary 3.2 (Antisymmetric Prime-Tower Signed-Area Law)**.** *For every integer base $p \geq 2$ and vertical-line abscissa $a \in (0,1)$, the total signed area of the pure-power curve tower $\mathcal{S}_p(a) := \sum_{k=1}^{\infty} \mathcal{A}_{\text{signed}}\big(t_{p,p^k}(a+ib)\big)$ converges absolutely to*

$$\mathcal{S}_p(a) = \frac{\pi(p-1)^2\big(p^{2a-2} - p^{-2a}\big)}{p^2\big(1-p^{2a-2}\big)^2\big(1-p^{-2a}\big)^2}. \tag{13}$$

Consequently, $\mathcal{S}_p(a)$ satisfies the reflection antisymmetry $\mathcal{S}_p(1-a) = -\mathcal{S}_p(a)$ for all $a \in (0,1)$, with $\mathcal{S}_p(a) < 0$ for $0 < a < \frac{1}{2}$, $\mathcal{S}_p(a) > 0$ for $\frac{1}{2} < a < 1$, and $\mathcal{S}_p(a) = 0$ if and only if $a = \frac{1}{2}$.

Proof. Let $r := p^{-2a} \in (p^{-2}, 1)$ and $q := p^{2a-2} \in (p^{-2}, 1)$, noting that $qr = p^{-2}$. Since $\big|\mathcal{A}_{\text{signed}}(t_{p,p^k}(a+ib))\big| = O(k\, r^k)$ and $0 < r < 1$, summing Equation (10) over $k \geq 1$ via $\sum_{k=1}^{\infty} r^k = \frac{r}{1-r}$ and $\sum_{k=1}^{\infty} k\, r^k = \frac{r}{(1-r)^2}$ gives

$$\begin{aligned}\mathcal{S}_p(a) &= \frac{\pi(p-1)^2 q}{(1-q)^2}\left(\frac{r}{1-r} - \frac{(1-q)r}{(1-r)^2}\right) \\ &= \frac{\pi(p-1)^2 qr}{(1-q)^2(1-r)^2}\big((1-r)-(1-q)\big) = \frac{\pi(p-1)^2(q-r)}{p^2(1-q)^2(1-r)^2},\end{aligned}$$

proving Equation (13). Under $a \mapsto 1-a$, $q = p^{2a-2}$ and $r = p^{-2a}$ swap places, reversing the sign of $q-r$ while leaving $p^2(1-q)^2(1-r)^2 > 0$ invariant, so $\mathcal{S}_p(1-a) = -\mathcal{S}_p(a)$. Finally, since $p > 1$, $p^{2a-2} - p^{-2a}$ has the same sign as $(2a-2) - (-2a) = 4(a - \frac{1}{2})$, which is negative on $(0, \frac{1}{2})$, positive on $(\frac{1}{2}, 1)$, and zero exclusively at $a = \frac{1}{2}$. □

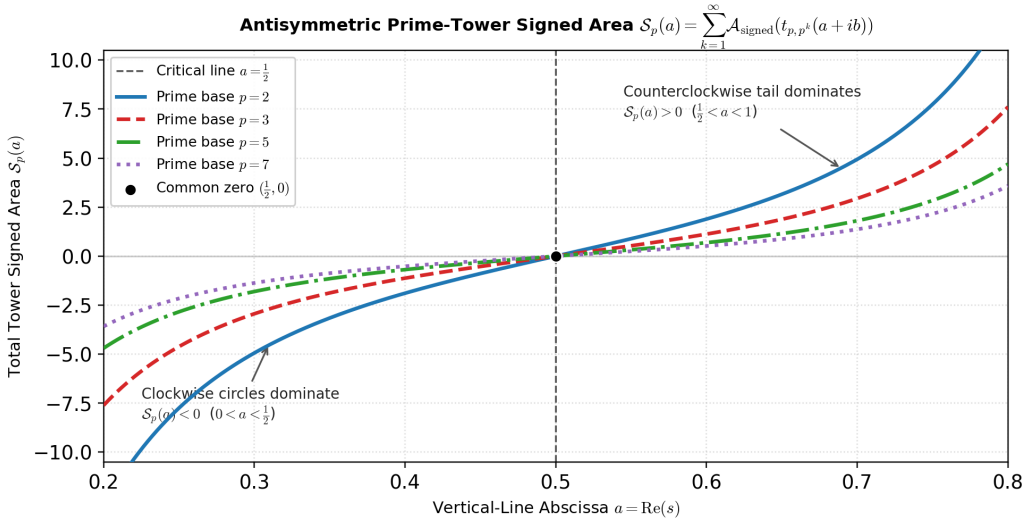


Figure 2: Total pure-power signed area $\mathcal{S}_p(a) = \sum_{k=1}^{\infty} \mathcal{A}_{\text{signed}}(t_{p,p^k}(a+ib))$ across $a \in [0.20, 0.80]$ for prime bases $p \in \{2,3,5,7\}$. Every prime tower is strictly negative on $0 < a < \frac{1}{2}$ (clockwise epicycles dominant), strictly positive on $\frac{1}{2} < a < 1$ (counterclockwise tail dominant), antisymmetric under $a \leftrightarrow 1-a$, and crosses zero uniquely on the critical line $a = \frac{1}{2}$.

Inspecting the double sum behind Corollary 3.2,

$$\mathcal{S}_p(a) = \pi(p-1)^2 \sum_{k=1}^{\infty} \sum_{m=1}^{\infty} (m-k)\, p^{-2ka-2m(1-a)}, \tag{14}$$

makes the structural mechanism behind this zero-crossing transparent. The harmonic winding factor $(m-k)$ is antisymmetric under exchanging the Dirichlet index k (governed by p^{-ks}) with the exterior prefactor index m (governed by $p^{m(s-1)}$), whereas the squared-modulus weight $p^{-2ka-2m(1-a)}$ becomes symmetric in (k,m) if and only if $a = 1-a$, i.e., $a = \frac{1}{2}$.

4 Conclusion

Comparing the unexpanded and power-series representations of $(1-p^{1-s})^{-1}$ highlights how two elementary faces of the same normalization expose complementary geometric structures inside $\zeta(s)$ across $0 < \mathrm{Re}(s) < 1$. Keeping $(1-p^{1-s})^{-1}$ intact preserves the closed degree-$2k$ algebraic curves $t_{p,p^k}(\frac{1}{2}+ib)$ over $\mathbb{Z}[x,y]$, their Blaschke elliptic perimeters, and the prime-versus-composite dichotomy established in [6, 7]. Expanding $(1-p^{1-s})^{-1} = -\sum_{m=1}^{\infty} p^{m(s-1)}$ and distributing it termwise instead resolves each pure-power trajectory into $k-1$ clockwise rotors, a motionless real-axis center-of-mass anchor $+(p-1)p^{-k}$, and an infinite counterclockwise tail. Through Green's theorem and Parseval's identity, that counter-rotating decomposition explains both how the Bernoulli lemniscate $t_4(\frac{1}{2}+ib)$ is pinched and area-balanced index-by-index and why $\mathrm{Re}(s) = \frac{1}{2}$ is the unique vertical line in the critical strip where $t_4(a+ib)$ and every prime pure-power tower achieve exact signed-area conservation.

References

[1] T. M. Apostol, *Introduction to Analytic Number Theory*, Undergraduate Texts in Mathematics, Springer-Verlag, New York, 1976.

[2] H. M. Edwards, *Riemann's Zeta Function*, Academic Press, New York, 1974.

[3] L. Euler, "Remarques sur un beau rapport entre les séries des puissances tant directes que réciproques," *Mémoires de l'Académie des Sciences de Berlin*, vol. 17, pp. 83–106, 1768 (read 1749); reprinted in *Opera Omnia*, Series 1, vol. 15, pp. 70–90.

[4] S. R. Garcia, J. Mashreghi, and W. T. Ross, *Finite Blaschke Products and Their Connections*, Springer Monographs in Mathematics, Springer, Cham, 2018.

[5] T. H. Gronwall, "Some remarks on conformal representation," *Annals of Mathematics*, Second Series, vol. 16, no. 1/4, pp. 72–76, 1914.

[6] R. Hackbarth, "Characterizing the Critical Line via Normalized Dirichlet Eta Terms: Concentric Circles, a Bernoulli Lemniscate, and Integer Algebraic Curves," preprint, 2026, https://zenodo.org/records/24325291.

[7] R. Hackbarth, "Plane Algebraic Curve Families from Normalized Zeta Series: Prime-Base Extensions and Composite Breakdown," preprint, 2026, https://zenodo.org/records/24332600.

[8] H. Hilton, *Plane Algebraic Curves*, Clarendon Press, Oxford, 1920.

[9] A. Hurwitz, "Sur quelques applications géométriques des séries de Fourier," *Annales scientifiques de l'École Normale Supérieure*, Série 3, vol. 19, pp. 357–408, 1902.

[10] J. D. Lawrence, *A Catalog of Special Plane Curves*, Dover Publications, New York, 1972.

[11] T. Needham, *Visual Complex Analysis*, Clarendon Press, Oxford, 1997.

[12] E. C. Titchmarsh, *The Theory of the Riemann Zeta-Function*, 2nd ed., edited and with a preface by D. R. Heath-Brown, Clarendon Press, Oxford, 1986.